J. Fluid Mech. (2001), *vol.* 431, *pp.* 433–443. Printed in the United Kingdom

Statistical evidence of hairpin vortex packets in wall turbulence

By K. T. CHRISTENSEN AND R. J. ADRIAN

Laboratory for Turbulence and Complex Flow, Department of Theoretical and Applied Mechanics, University of Illinois, Urbana, IL 61801, USA

(Received 14 October 2000 and in revised form 15 December 2000)

The structure of velocity in the outer region of turbulent channel flow ($y^+ \gtrsim 100$) is examined statistically to determine the average flow field associated with spanwise vortical motions. Particle image velocimetry measurements of the streamwise and wall-normal velocity components are correlated with a vortex marker (swirling strength) in the streamwise–wall-normal plane, and linear stochastic estimation is used to estimate the conditional average of the two-dimensional velocity field associated with a swirling motion. The mean structure consists of a series of swirling motions located along a line inclined at 12°–13° from the wall. The pattern is consistent with the observations of outer-layer wall turbulence in which groups of hairpin vortices occur aligned in the streamwise direction. While the observational evidence for the aforementioned model was based upon both experimental and computational visualization of instantaneous structures, the present results show that, on average, the instantaneous structures occur with sufficient frequency, strength, and order to leave an imprint on the statistics of the flow as well. Results at $Re_\tau = 547$ and 1734 are presented.

1. Introduction

The structure of turbulent flow near a boundary has been studied extensively over the past decades (for a comprehensive review of this history, the reader should consult Robinson 1991 and, more recently, the collection edited by Panton 1997). Moreover, there is broad evidence that a vortical structure qualitatively similar to the 'horseshoe vortex' proposed by Theodorsen (1952) does exist in wall turbulence. (Throughout this paper, 'hairpin vortex' is used in a modern sense to include quasi-streamwise vortices connected to inclined necks and a spanwise arch that may have the shape of a hairpin, horseshoe, cane, or randomly perturbed variant. The essential feature is that the arch is strong enough to induce a local ejection event under it. A more complete discussion can be found in Adrian, Meinhart & Tomkins 2000, referred to herein as AMT.) At low Reynolds number, Smith (1984) reported the existence of hairpin loops and proposed an organized alignment of these structures in the streamwise direction. This near-wall model is consistent with the long streamwise extent of low-speed streaks and the observation of multiple ejections of low-speed fluid within a given bursting event. Smith *et al.* (1991) extended this work to argue that hairpins can actually regenerate from an existing vortex under the proper conditions. This lends support to the proposition that there exists a coherent ordering of hairpin vortices in wall turbulence.

More recently, Zhou *et al.* (1997, 1999) studied the evolution of an initial vortical structure qualitatively similar to a hairpin vortex in a low Reynolds number direct

numerical simulation (DNS) of turbulent channel flow. Given sufficient strength of the initial structure, multiple hairpins were observed both upstream and downstream of this structure. These newly formed structures mature and then generate additional hairpin vortices. This sequence of autogenerated events was generally consistent with those proposed by Smith *et al.* (1991). Additionally, Zhou *et al.* (1999) found clear evidence indicating that non-symmetric vortices have stronger growth rates, and are, therefore, preferred. Finally, Zhou *et al.* (1997) compared the velocity patterns seen in the three-dimensional DNS data with two-dimensional particle image velocimetry (PIV) velocity measurements in a turbulent boundary layer. This comparison led to the identification of a two-dimensional hairpin vortex signature which was used to identify the 'imprints' of the three-dimensional structures in the two-dimensional experimental data.

Although the work cited above supports the idea that hairpin vortices align in a coherent manner, it was performed at relatively low Reynolds numbers. Thus, the conclusions drawn from this body of research are, in general, mostly applicable to only the near-wall region of moderate to high Reynolds number situations. The body of knowledge about the structure of the outer layer of wall turbulence at Reynolds numbers that are not low is much more sparse compared to that of the near-wall region. However, it has been established that the outer layer does contain inclined structures which are associated with ejections and sweeps (Brown & Thomas 1977; Chen & Blackwelder 1978; Head & Bandyopadhyay 1981). Further, Head & Bandyopadhyay (1981) report the existence of vortex loops, horseshoe, and hairpin structures in smoke visualizations of a zero-pressure-gradient turbulent boundary layer at higher Reynolds numbers ($Re_\theta \leqslant 17\,500$). They also successfully visualize ramp-like patterns at the outer-most edge of the boundary layer, and propose this to be the imprint of groups of hairpin vortices inclined away from the wall at a shallow angle (15°–20°). Bandyopadhyay (1980) developed a simple model that predicts this angle to be 18°.

Recent PIV measurements in a turbulent boundary layer by AMT provide strong evidence that structures consistent with hairpin vortices occur throughout the outer layer at both low and high Reynolds numbers. They also showed that the vortices actually align coherently in the streamwise direction, creating a larger-scale coherent motion referred to as a *hairpin vortex packet*. The PIV data permitted visualization of the packets within the interior of the boundary layer, and this evidence showed that the packets occur throughout the outer region in a hierarchy of scales. AMT proposed a model whereby packets of multiple hairpin vortices are created at the wall and grow to occupy the entire boundary layer. This model provides a link between the evidence supporting the existence of vortex organization in both the near-wall and outer layer of the flow. The hairpin packet is characterized by two distinct features:

(*a*) a series of hairpin vortices aligned in the streamwise direction, with their heads forming an interface inclined away from the wall at angles between 12° and 20°;

(*b*) a region of relatively uniform, low-momentum fluid lying beneath the inclined interface created by the heads of the vortices due to the collective induction of the vortices.

Vortex packets can contain ten or more individual vortices which propagate as a coherent entity, and they can extend to twice the outer length scale in the streamwise direction. Due to the two-dimensional nature of the experimental technique used by AMT, the character of the vortex organization in the spanwise direction could not be observed directly. However, by combining visualizations of the three-dimensional structure found in DNS, which are necessarily low Reynolds number, with the two-

dimensional data taken at significantly higher Reynolds number, a picture emerges that generally supports the hairpin packet model.

Since vortex organization in the outer region is commonly observed in instantaneous realizations of wall turbulence (including the atmospheric boundary layer (Hommema & Adrian 2001)), it is conjectured that the vortex packet is a dominant and robust feature of wall-bounded turbulent flows within the region where structural similarity exists (the structural character of channel, pipe, and boundary-layer flows is quite similar below $y/h \sim 0.6$, i.e. below the wake region). If this is indeed the case, these structures (both the vortices and the packets) should leave their imprint upon the statistics of the flow in some manner. However, spectra and two-point correlation functions to date seem to indicate the absence of such structure. The present work reports evidence that the structure of the two-point spatial correlations contains a clear picture of organized turbulent motion that is consistent with the pattern associated with a hairpin vortex packet.

2. Experiment

The experiments which form the basis of this work are performed in turbulent channel flow. The working fluid is air and the facility is driven by a centrifugal blower. The apparatus has a channel cross-section of $5.08\,\text{cm} \times 51.44\,\text{cm}$ ($2h \times w$, where h and w are the half-height and width of the channel, respectively) and has a development length of $216h$. Particle image velocimetry is used to measure two-dimensional velocity (u, v) fields in the streamwise–wall-normal (x, y)-plane along the channel centreline. The measurement domain is $h \times h$ and 3500 independent velocity realizations are acquired at each of three Reynolds numbers: $Re_\tau = u_\tau h/\nu = 547, 1133$, and 1734. The mean velocity, RMS velocity, and Reynolds stress profiles over this range of Reynolds numbers are consistent with fully developed turbulent channel flow. Further experimental details can be found in Christensen (2001).

3. Instantaneous structure

Before introducing the instantaneous evidence of vortex organization in the outer layer, it is worthwhile to discuss the vortex identification tools used to interpret instantaneous velocity realizations. The vortex definition offered by Kline & Robinson (1989) is adopted here. It states that a vortex is defined as a region of concentrated vorticity around which the pattern of streamlines is roughly circular when viewed in a frame moving with the centre of the vortex. In two-dimensional velocity fields, a vortex is visualized properly when the convection velocity of the vortex is removed from the field. In this frame of reference, the velocity vector pattern will consist of closed streamlines in the spirit of the Kline & Robinson (1989) definition. Further, rather than using vorticity to identify vortex cores, a different vortex identification technique, referred to as swirling strength, is used in the present work. Swirling strength, λ_{ci} (i is not an index in this definition, but an abbreviation for the word 'imaginary'), is the imaginary portion of the complex eigenvalue of the local velocity gradient tensor and is an unambiguous measure of rotation (Zhou *et al.* 1999). Unlike vorticity, swirling strength does not highlight regions of intense shear and it has been shown to be an effective identifier of *true* vortex cores (Adrian, Christensen & Liu 2000). In addition, swirling strength yields patterns that are very similar to those found using the vortex identification technique of Jeong & Hussain (1995). Since complex eigenvalues of the

velocity gradient tensor occur in conjugate pairs, the positive imaginary portion is assigned to λ_{ci}. Therefore, by convention, $\lambda_{ci} \geqslant 0 \forall \boldsymbol{x}$.

To illustrate the dominance of the vortex organization in the outer layer and also the apparent Re-independence of this behaviour, results from the $Re_\tau = 547$ and $Re_\tau = 1734$ datasets will be presented. Figure 1 shows typical instantaneous PIV velocity fields in the streamwise–wall-normal plane of the channel at (*a*) $Re_\tau = 547$ and (*b*) $Re_\tau = 1734$. A constant convection velocity ($U_c = 0.85U_{CL}$ in both cases, where U_{CL} is the centreline velocity) is removed from each field to reveal those vortex structures whose cores are advecting at this speed. Contours of swirling strength (λ_{ci}) are shown in the background of the velocity field to highlight the locations of vortex cores. The fields contain many examples of vortex cores interpreted to be associated with the heads of hairpin vortices advecting in the streamwise direction. A lifting of low-speed fluid away from the wall (referred to as a Q_2 event in the nomenclature introduced by Wallace, Eckelmann, & Brodkey 1972; Willmarth & Lu 1972) just under and upstream of the hairpin head is consistent with the hairpin vortex signature introduced by Zhou *et al.* (1997) and AMT. A single vortex packet is visible in each realization and the outer edge of each packet is roughly defined by the dashed line superimposed upon the velocity field. At $Re_\tau = 547$, four vortices are aligned in the field of view and the angle of inclination of this packet, relative to the wall, is approximately 17°. At $Re_\tau = 1734$, five vortices are aligned in the field of view, and the angle of inclination of this packet is 16°. The physics of these instantaneous realizations is entirely consistent with the results of Zhou *et al.* (1997, 1999), and AMT, indicating that vortex organization is a common feature in the outer region of wall-bounded turbulent flows. The spacing between successive vortices is a fundamental parameter of the packets, but studies of instantaneous realizations have not been able to define this spacing unambiguously.

We are not aware of any other propositions in the literature that account for the vortex organization seen in the outer layer as simply as the hairpin packet model. Further, the results presented here and introduced by Zhou *et al.* (1997, 1999), and AMT are not inconsistent with the work in which quasi-streamwise vortices are thought to be the dominant near-wall structure (Schoppa & Hussain 1997; Brooke & Hanratty 1993; Heist, Hanratty & Na 2000, among others). In fact, near the wall, asymmetric hairpin-like structures, as defined in AMT, are consistent (apart from naming convention) with quasi-streamwise vortices arched slightly in the spanwise direction (similar to the arch vortices studied by Heist *et al.* 2000, for example). In addition, there is no apparent inconsistency because the latter body of research cited above only focused upon the very near-wall region of the flow ($y^+ \lesssim 60$), while the present work focuses upon the *outer region* (the logarithmic layer and beyond).

4. Statistical analysis

Although the vast majority of instantaneous realizations are consistent with the notion that hairpin vortex organization is a common feature of the outer region, the parameters of these patterns must be investigated statistically. This organization should be evident within the statistics of the flow if these structures have a consistent character (spacing of vortex heads and angle of inclination). If, however, variations between instantaneous realizations of packets are large enough, the imprint can be destroyed in the averaging process. Therefore, one could pose the question: *Given the presence of a single spanwise vortex core (believed to be associated with the head of a hairpin vortex), what is the average fluctuating velocity field associated with this*

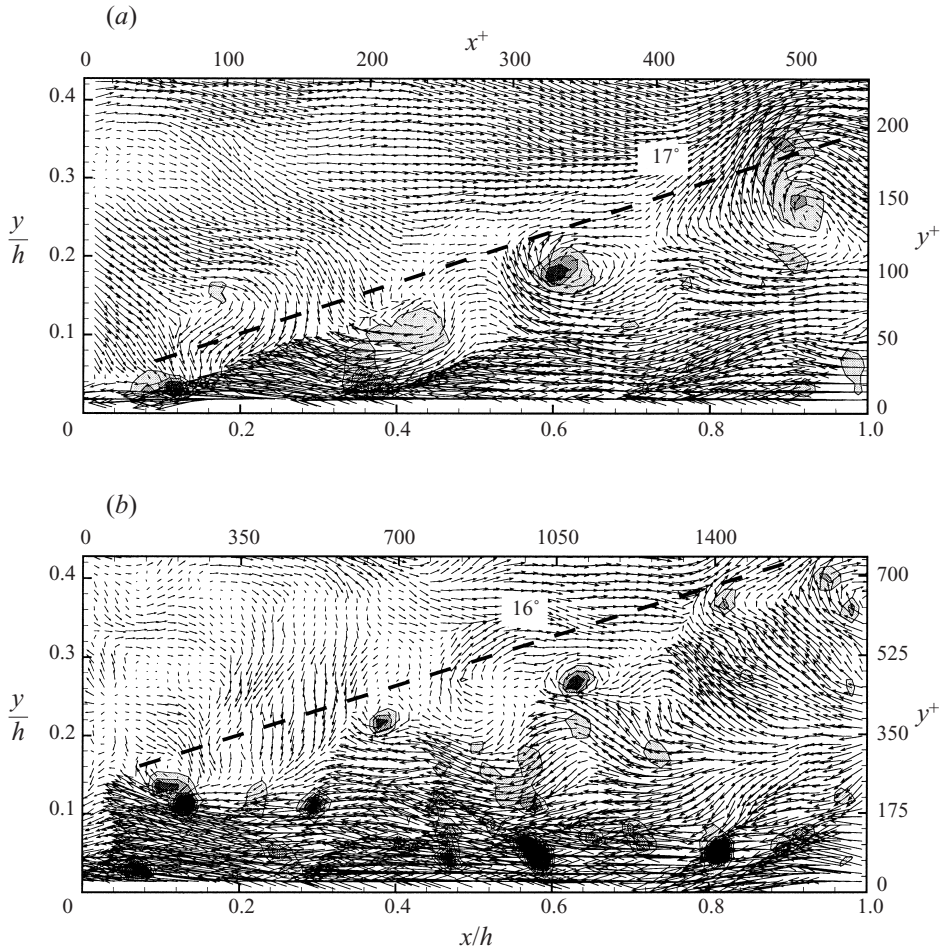

FIGURE 1. Instantaneous velocity realizations in turbulent channel flow with a constant convection velocity, $U_c = 0.85U_{CL}$, removed. (*a*) $Re_\tau = 547$; (*b*) $Re_\tau = 1734$. Contours of swirling strength are shown in the background to highlight the location of vortex cores.

physical event? The best estimate of the average velocity field is the conditional average of the velocity field given the presence of a vortex core (represented by λ_{ci}): $\langle \boldsymbol{u}'(\boldsymbol{x}')|\lambda_{ci}(\boldsymbol{x})\rangle$, where $\boldsymbol{x} = (x, y)$. Since direct computation of this conditional average is impractical, it must be estimated in some fashion. Stochastic estimation of conditional averages minimizes the error between the conditional average and the estimate in a mean-square sense (Adrian 1988) (the reader is directed to this reference for a comprehensive discussion of stochastic estimation). Studies of many types of turbulent fields have shown that linear estimates are surprisingly accurate and relatively simple to form (Adrian, Moin & Moser 1987). The conditional average postulated above can be estimated in a linear fashion as

$$\langle u_j'(\boldsymbol{x}')|\lambda_{ci}(\boldsymbol{x})\rangle \approx L_j\lambda_{ci}(\boldsymbol{x}), \tag{4.1}$$

where the kernel L_j is determined by minimizing the mean-square error between the estimate and the conditional average (recall that i is not an index). This error

minimization gives

$$\langle u_j'(\boldsymbol{x}')|\lambda_{ci}(\boldsymbol{x})\rangle \approx \frac{\langle \lambda_{ci}(\boldsymbol{x})u_j'(\boldsymbol{x}')\rangle}{\langle \lambda_{ci}(\boldsymbol{x})\lambda_{ci}(\boldsymbol{x})\rangle}\lambda_{ci}(\boldsymbol{x}). \tag{4.2}$$

The estimate of the conditional average is only a function of unconditional two-point correlation data. Therefore, (4.2) allows one to reconstruct the average velocity behaviour associated with a given value of λ_{ci} at $\boldsymbol{x}$. However, it is important to note that since the event of the conditional average is simply a single scalar value, it is sufficient to specify $\lambda_{ci} > 0$ (a non-trivial event). That is, the character of the estimate of the conditionally averaged velocity field remains the same for all values of $\lambda_{ci} > 0$, since the magnitudes of the velocity vectors within a given estimate are simply amplified or attenuated by the chosen value of λ_{ci}. Therefore, if one specifies $\lambda_{ci} = \lambda_{ci}^a$ and computes an estimate, and then specifies $\lambda_{ci} = \lambda_{ci}^b$ ($\lambda_{ci}^b \neq \lambda_{ci}^a$) and computes another estimate, these estimates will be identical except for a constant scaling factor defined by the ratio of λ_{ci}^a and λ_{ci}^b. Since thresholding of λ_{ci} is not necessary, the estimate remains objective beyond the choice of event type and event location in the wall-normal direction.

4.1. *Correlation functions*

As is indicated by (4.2), the two-point correlation functions between swirling strength and velocity are necessary for estimation of the conditionally averaged velocity field given a vortex core. The two-point correlation between swirling strength and the streamwise velocity fluctuation, for example, is defined as

$$R_{\lambda u}(r_x, y) = \frac{\langle \lambda_{ci}(x, y_{\mathrm{ref}})u'(x + r_x, y)\rangle}{\sigma_\lambda(y_{\mathrm{ref}})\sigma_u(y)}, \tag{4.3}$$

where σ refers to the root-mean square of the given quantity. Again, recall that $\lambda_{ci} \geqslant 0$ $\forall\ \boldsymbol{x}$, so $R_{\lambda u}$ and $R_{\lambda v}$ retain the sign of u' and v', respectively. Therefore, the correlation functions embody structural information in the spirit of Bandyopadhyay & Watson (1988). In this study, $R_{\lambda u}$ and $R_{\lambda v}$ are formed from 3500 statistically independent realizations at each Reynolds number, yielding correlation functions in which the statistical sampling errors are minimal.

Figures 2 and 3 illustrate $R_{\lambda u}$ and $R_{\lambda v}$ for $y_{\mathrm{ref}}/h = 0.15$ at $Re_\tau = 547$ ($y_{\mathrm{ref}}^+ = 83.6$) and $Re_\tau = 1734$ ($y_{\mathrm{ref}}^+ = 256.0$), respectively. Both the streamwise and wall-normal correlation functions are strongest near the reference line (as expected). $R_{\lambda u}$ is negative below and positive above y_{ref}, while $R_{\lambda v}$ is positive to the left of and negative to the right of $r_x = 0$. This behaviour is entirely consistent with the correlation between a region of strong swirling strength and the velocity vector pattern of a hairpin vortex head which, by definition, has a clockwise rotation. The wall-normal correlation is stronger upstream than downstream of $r_x = 0$, and the streamwise correlation is stronger below y_{ref} than above it, which is consistent with a Q_2 event induced by the head and leg(s) of the vortex. Additionally, a large-scale, inclined interface is noted in both the streamwise and wall-normal correlations. The correlation beneath this interface is negative in $R_{\lambda u}$ and positive in $R_{\lambda v}$. This behaviour is consistent with the conjecture that the flow is dominated by a series of hairpin vortices aligned in the streamwise direction, whose heads lie along a line inclined away from the wall, beneath which exists a region of relatively uniform low-momentum fluid created by the collective induction of the vortices. This conjecture is valid even if the vortices are not complete hairpins, but rather cane-like vortices, for example, which have a single leg connected to the spanwise-oriented head. It is also worth noting that the

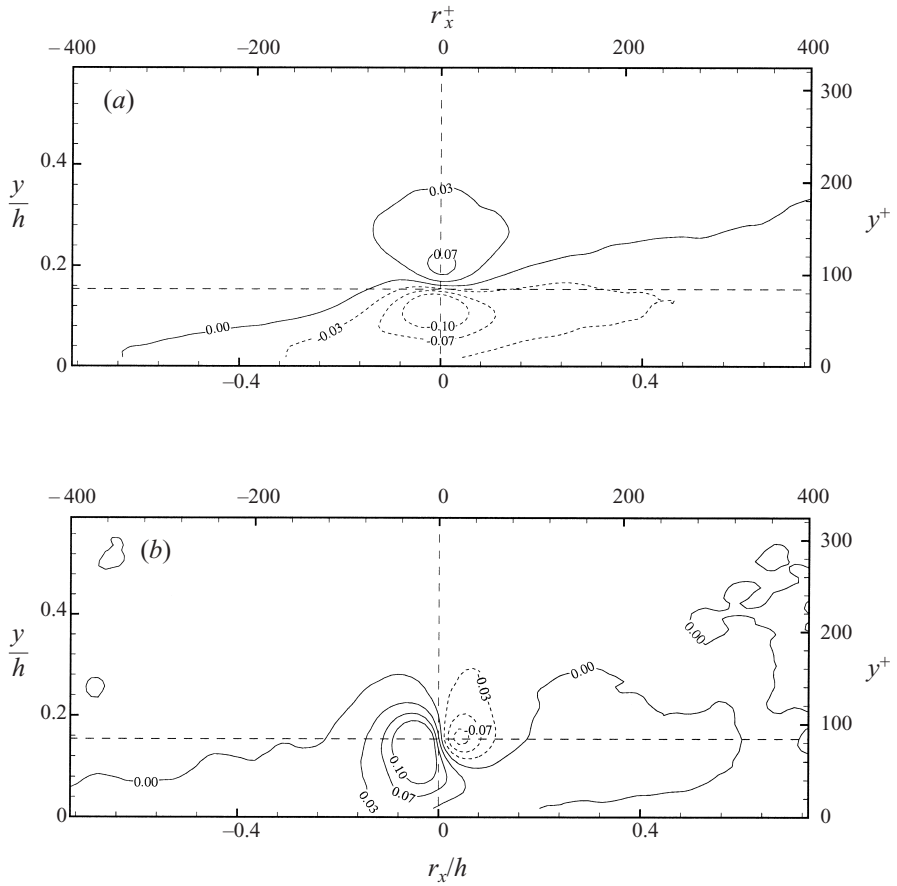

FIGURE 2. Two-point correlations between velocity and swirling strength at $Re_\tau = 547$ for $y^+_{\mathrm{ref}} = 83.6$ ($y_{\mathrm{ref}}/h = 0.15$). (*a*) $R_{\lambda u}$; (*b*) $R_{\lambda v}$. The horizontal dashed line indicates the location of y_{ref}.

behaviour of $R_{\lambda u}$ and $R_{\lambda v}$ at $Re_\tau = 547$ and $Re_\tau = 1734$ shows definite similarity, indicating that this large-scale behaviour is relatively insensitive to Reynolds number.

4.2. *Stochastic estimation results*

The two-point correlations between swirling strength and velocity presented in the previous section are used to perform the stochastic estimation of $\langle u_j'(\boldsymbol{x}')|\lambda_{ci}(\boldsymbol{x})\rangle$. Figure 4(*a*) illustrates the estimate of the conditionally averaged velocity field at $Re_\tau = 547$ given $\lambda_{ci}(\boldsymbol{x}) = \sigma_\lambda(y_{\mathrm{ref}}/h = 0.15)$. The length of each vector was forced to unity by normalizing each with its magnitude. This is necessary because the stochastically estimated velocity field is strongest around the event point, and this strength tends to obscure weaker motions away from the event location. As expected, a distinct swirling motion is centred at the event location (shown by a solid circle). This swirling motion is consistent with the key features established in the hairpin vortex signature: closed streamlines representing the head of the vortex and a Q_2 event just upstream and below the head produced by the induction of the hairpin head and leg(s). Swirling motions (labelled A–C) are also evident both upstream and downstream of the event location. They lie along a line which is inclined from

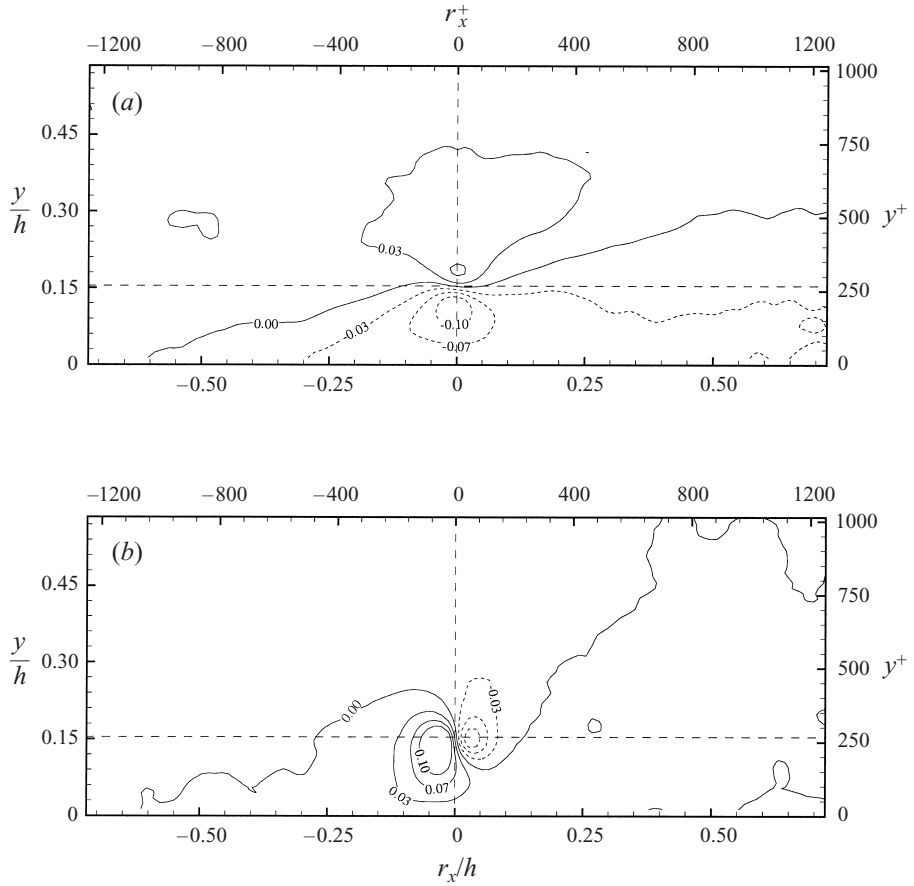

FIGURE 3. As figure 2 but at $Re_\tau = 1734$ for $y_{\mathrm{ref}}^+ = 256.0$.

the wall. A swirling motion (A) is present upstream of the event location, while two distinct swirling patterns (B, C) are evident downstream of the event location. This line of swirling patterns is inclined away from the wall at an angle of 13°. It is worth noting that the swirling patterns both upstream and downstream of the event location appear slightly smeared in the streamwise direction. This 'smeared' appearance is probably due to fluctuation of the vortex spacing about its mean. If the vortex spacing were fixed from packet to packet, the swirling motions would appear much more defined and circular. However, since the streamwise spacing of the vortices naturally varies slightly from packet to packet, this variation tends to broaden the extent of the average swirling motions in the streamwise direction.

The stochastic estimate of the conditionally averaged velocity field at $Re_\tau = 1734$ given $\lambda_{ci}(\boldsymbol{x})=\sigma_\lambda(y_{\mathrm{ref}}/h = 0.15)$ appears in figure 4(*b*). As expected, a strong swirling motion is centred at the event location (shown by a solid circle) and is consistent with the hairpin vortex signature. However, just as in the low Reynolds number result, additional swirling motions (labelled A–C) are also evident both upstream and downstream of the event location and lie along a line which is inclined from the wall at an angle of 14°.

The qualitative similarity between the stochastically estimated velocity fields of figure 4 and the instantaneous fields shown in figure 1 is clear. The angle of incli-

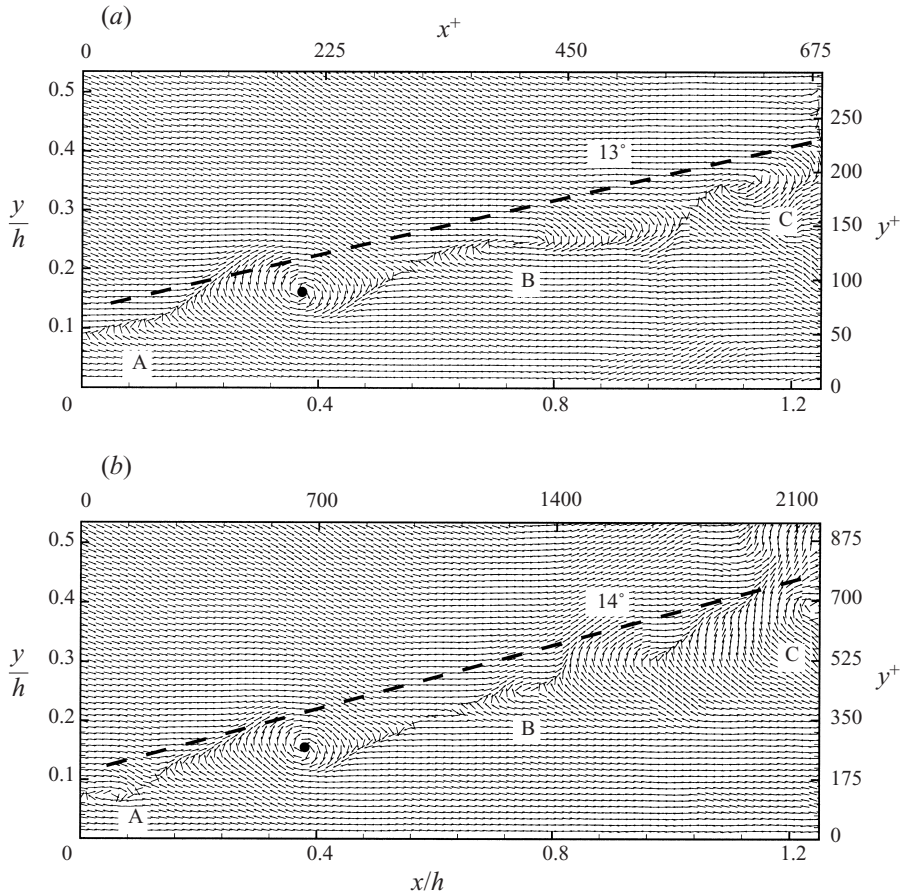

FIGURE 4. Linear stochastic estimation of $\langle u_j'(\boldsymbol{x}')|\sigma_\lambda(y_{\mathrm{ref}}/h = 0.15)\rangle$. The location of the swirling strength event is indicated by a solid circle. (*a*) $Re_\tau = 547$ ($y^+_{\mathrm{ref}} = 83.6$); (*b*) $Re_\tau = 1734$ ($y^+_{\mathrm{ref}} = 256.0$). Vectors have been normalized to unity by their respective magnitudes to highlight swirling motions away from the event location. Comparison to the instantaneous fields shown in figure 1 indicates that the vortex organization in the outer region is a dominant and robust feature.

nation of the stochastically estimated fields is similar to those in the instantaneous realizations, as is the vortex spacing. The ordering of the swirling patterns in the estimate of the conditionally averaged velocity fields is telling, because it is entirely consistent with the hairpin vortex packet model of AMT. Further, the estimates of the conditionally averaged velocity illustrate how dominant, persistent, and well-ordered the vortex organization truly is in the outer region. At the highest Reynolds number, it is quite surprising that the vortex organization is able to survive the averaging process since the range of length scales is three times broader than the range of the $Re_\tau = 547$ case. It is worth noting that the mean spacing of the swirling motions are essentially the same at $Re_\tau = 547$ and $Re_\tau = 1734$ when scaled with the outer length scale, h. This implies a Reynolds number insensitivity of vortex spacing, as was also suggested in the instantaneous realizations of figure 1.

Given the robust vortex organization presented here, it is logical to consider the possibility of packet organization of some form. For example, evidence exists that the largest packets may align to form very large-scale motions in turbulent pipe flow

Kim & Adrian 1999. Also, one can imagine packets nesting within one another and propagating coherently as an even larger-scale coherent entity. If so, this behaviour should be present within the stochastically estimated velocity fields in figure 4. However, careful examination of these fields over a larger field of view than shown here does not indicate any evidence of packet nesting. This is not entirely surprising, since packets of different sizes would tend to travel at different velocities (AMT). Therefore, the packets would have no fixed spatial relationship. It is still possible, however, that hairpin packets might propagate coherently one behind another (as a *train* of packets). Unfortunately, the field of view of the measurements presented here is not large enough to consider this possibility.

5. Summary and conclusions

Statistical evidence is presented which supports the notion that the outer layer of wall turbulence is populated by spatially coherent groups of vortices. The organization of the vortices leaves a distinct imprint upon the statistics of the flow at both low and high Reynolds numbers. Near y_{ref} and $r_x = 0$, the two-point correlations between swirling strength and the streamwise and wall-normal velocities are consistent with the head of a hairpin vortex. Additionally, both correlation functions show a large-scale behaviour that is consistent with the statistical signature of hairpin vortex packets embedded within the flow. This conjecture is further supported by the estimate of the conditionally averaged velocity field given a vortex core, which shows multiple swirling motions inclined away from the wall and aligned in the streamwise direction. This vortex organization is consistent with the hairpin vortex packets seen in the work of Zhou *et al.* (1997, 1999), and AMT. Although the outer-layer vortex organization is not inconsistent with the current body of literature, we know of no other propositions in the literature that can explain this striking phenomenon as simply as the hairpin vortex packet.

The support of the National Science Foundation and the Air Force Office of Scientific Research is gratefully acknowledged. The first author was partially supported by a National Science Foundation Graduate Fellowship.

REFERENCES

Adrian, R. J. 1988 Linking correlations and structure: Stochastic estimation and conditional averaging. In *Zoran P. Zaric Memorial International Seminar on Near-Wall Turbulence*. Dubrovnik, Yugoslavia: Hemisphere.

Adrian, R. J., Christensen, K. T. & Liu, Z.-C. 2000 Analysis and interpretation of instantaneous turbulent velocity fields. *Exps. Fluids* **29**, 275–290.

Adrian, R. J., Meinhart, C. D. & Tomkins, C. D. 2000 Vortex organization in the outer region of the turbulent boundary layer. *J. Fluid Mech.* **422**, 1–54 (referred to herein as AMT).

Adrian, R. J., Moin, P. & Moser, R. D. 1987 Stochastic estimation of conditional eddies in turbulent channel flow. In *CTR Proc. of the Summer Program*, pp. 7–19.

Bandyopadhyay, P. 1980 Large structure with a characteristic upstream interface in turbulent boundary layer. *Phys. Fluids* **23**, 2326–2327.

Bandyopadhyay, P. R. & Watson, R. D. 1988 Structure of rough-wall turbulent boundary layers. *Phys. Fluids* **31**, 1877–1883.

Brooke, J. W. & Hanratty, T. J. 1993 Origin of turbulence-producing eddies in a channel flow. *Phys. Fluids* A **5**, 1011–1022.

Brown, G. R. & Thomas, A. S. W. 1977 Large structure in a turbulent boundary layer. *Phys. Fluids* **20**, S243–251.

Chen C. H. P. & Blackwelder, R. F. 1978 Large-scale motion in a turbulent boundary layer: A study using temperature contamination. *J. Fluid Mech.* **89**, 1–31.

Christensen, K. T. 2001 Experimental investigation of acceleration and velocity fields in turbulent channel flow. PhD thesis, Department of Theoretical and Applied Mechanics, University of Illinois at Urbana-Champaign.

Head, M. R. & Bandyopadhyay, P. 1981 New aspects of turbulent boundary-layer structure. *J. Fluid Mech.* **107**, 297–338.

Heist, D. K., Hanratty, T. J. & Na, Y. 2000 Observations of the formation of streamwise vortices from arch vortices. *Phys. Fluids* **12**, 2965–2975.

Hommema, S. E. & Adrian, R. J. 2001 Structure of wall-eddies at $Re_s \geqslant 10^6$. In *Selected Papers from the 10th Intl Symp. of Laser Techniques to Fluid Mechanics, Lisbon, Portugal* (to appear).

Jeong, J. & Hussain, F. 1995 On the identification of a vortex. *J. Fluid Mech.* **285**, 69–94.

Kim, K. C. & Adrian, R. J. 1999 Very large-scale motion in the outer layer. *Phys. Fluids* **11**, 417–422.

Kline, S. J. & Robinson, S. K. 1989 Quasi-coherent structures in the turbulent boundary layer. Part 1: Status report on a community-wide summary of the data. In *Near Wall Turbulence* (ed. S. J. Kline & N. H. Afgan), pp. 218–247. Hemisphere.

Panton, R. L. 1997 *Self-Sustaining Mechanisms of Wall Turbulence*. Southampton, UK: Computational Mechanics Publications.

Robinson, S. K. 1991 Coherent motions in the turbulent boundary layer. *Ann. Rev. Fluid Mech.* **23**, 601–639.

Schoppa, W. & Hussain, F. 1997 Genesis and dynamics of coherent structures in near-wall turbulence: A new look. In *Self-Sustaining Mechanisms of Wall Turbulence* (ed. R. L. Panton), chap. 16, pp. 385–422. Southampton, UK: Computational Mechanics Publications.

Smith, C. R. 1984 A synthesized model of the near-wall behavior in turbulent boundary layers. In *Proc. 8th Symp. on Turbulence*, pp. 299–325. Rolla, Missouri: Univ. Missouri-Rolla.

Smith, C. R., Walker, J. D. A., Haidari, A. H. & Sobrun, U. 1991 On the dynamics of near-wall turbulence. *Phil. Trans. R. Soc. Lond.* A **336**, 131–175.

Theodorsen, T. 1952 Mechanism of turbulence. In *Proc. 2nd Midwestern Conf. on Fluid Mech.*, pp. 1–19. Columbus, Ohio: Ohio State Univ.

Wallace, J. M., Eckelmann, H. & Brodkey, R. S. 1972 The wall region in turbulent shear flow. *J. Fluid Mech.* **54**, 39–48.

Willmarth, W. W. & Lu, S. S. 1972 Structure of the Reynolds stress near the wall. *J. Fluid Mech.* **142**, 121–149.

Zhou, J., Adrian, R. J., Balachandar, S. & Kendall, T. M. 1999 Mechanisms for generating coherent packets of hairpin vortices in channel flow. *J. Fluid Mech.* **387**, 353–396.

Zhou, J., Meinhart, C. D., Balachandar, S. & Adrian, R. J. 1997 Formation of coherent hairpin packets in wall turbulence. In *Self-Sustaining Mechanisms of Wall Turbulence* (ed. R. L. Panton), pp. 109–134. Southampton, UK: Computational Mechanics Publications.